VEGETATION PHENOLOGY, LAND-SURFACE COOLING, AND CLIMATE-RESPONSIVE AGRICULTURAL PLANNING IN NORTHEAST CHINA

Emily Jones

Vegetation phenology increasingly shapes regional land–atmosphere interactions in ways that matter for both climate science and climate-sensitive land management. Using long-term remote-sensing observations and fully coupled Weather Research and Forecasting simulations, this study quantifies how observed phenological shifts between the early 2000s and the late 2010s altered land-surface temperature across Northeast China, a major grain-producing region. The analysis focuses on the two dominant land-cover systems—temperate forests and croplands—and jointly evaluates timing shifts, seasonal thermal responses, and the biophysical pathways through which canopy change affected surface temperature. The results show that forests experienced earlier spring development, while croplands combined earlier green-up with delayed dormancy, producing a larger extension of the growing season in managed landscapes. The paired simulations indicate that these changes increased canopy development and strengthened vegetation–climate coupling, yielding more pronounced and more persistent cooling in croplands than in forests. Forest cooling was concentrated in May during rapid green-up, whereas cropland cooling was strongest in June, July, and September. Biophysical attribution indicates that reduced aerodynamic resistance was the dominant cooling pathway, with atmospheric feedback as the second most important contributor. Taken together, the findings establish that phenology is a material planning variable: in regions where agricultural calendars, land management, and climatic risk interact closely, shifts in canopy timing can measurably alter seasonal thermal conditions and should be incorporated into climate adaptation and land-use planning.

INTRODUCTION

Vegetation phenology is a central indicator of ecological response to climate change, but it is also a conse-quential regulator of land–atmosphere exchange. Changes in green-up timing, canopy development, peak greenness, and dormancy alter albedo, surface roughness, evapotranspiration, and the partitioning of available energy between latent and sensible heat [1, 10, 11, 13]. In temperature-limited systems, these changes can feed back to the regional climate by reshaping the seasonal pattern of land-surface temperature.

This interaction is especially important in regions where managed agricultural systems and natural vegetation coexist across large areas. In such settings, phenological shifts influence not only ecological functioning, but also planting and harvest windows, water demand, crop exposure to heat, and the design of climate adaptation strategies. Land-surface change is therefore not merely an environmental process; it is also a planning variable.

Northeast China is a particularly important case. It is one of the country's major grain-producing regions and has experienced pronounced warming, measurable phenological change, and strong land-cover contrasts between forests and croplands [12, 13, 18]. The regional question is not simply whether vegetation is changing, but whether changes in the timing and intensity of canopy development are materially altering seasonal surface temperature in ways that matter for agricultural management and regional planning.

To address that question, this study develops a fully integrated analysis of phenological control on land-surface cooling in Northeast China, combining long-term satellite observations, paired regional climate simulations, and biophysical pathway attribution within a single planning-oriented framework. The objective is not simply to document phenological change, but to quantify its thermal consequences, identify the dominant mechanisms, and clarify why those effects matter for agricultural and regional decision-making. The analysis is centered on three research questions:

1. How did phenology change from 2003 to 2020 in forests and croplands across Northeast China?

2. How did those observed shifts alter land-surface temperature across the seasonal cycle?

3. Which biophysical pathways most strongly mediated the temperature response, and what do those mechanisms imply for agricultural and regional planning?

The study makes three specific contributions. It quantifies contrasting phenological trajectories in forests and croplands, estimates the associated seasonal LST response under a controlled paired-simulation design, and translates the resulting mechanistic evidence into a bounded planning interpretation. In this way, phenology is treated not simply as a passive ecological signal, but as a dynamic component of the climatic operating environment within which planning decisions are made.

STUDY CONTEXT AND ANALYTICAL FRAMING

Northeast China spans approximately 1.24×10^6 km^2 and is characterized by a temperate continental monsoon climate, cold snowy winters, and warm, rainy summers. Forests and croplands together account for roughly 71% of the region's land cover, making the region well suited for comparative analysis of natural and managed vegetation systems [18]. Because the area is both climatically sensitive and agriculturally strategic, even modest changes in seasonal temperature regulation have implications for cropping calendars, resource management, and adaptation planning.

The analytical framing adopted here treats vegetation phenology as a planning-relevant land-surface process. Earlier green-up can lengthen the active growing season and enhance spring cooling, but it can also alter water balances and affect subsequent seasonal energy exchange. Delayed dormancy can extend canopy influence into late summer and autumn, potentially shifting the timing of surface cooling in cropland systems. These effects are not merely academic: they can influence when thermal stress emerges, when water demand intensifies, and how planners interpret seasonal risk across agricultural landscapes.

```
┌──────────────────────────┐          ┌──────────────────────────┐
│  MODIS phenology metrics │ ───────▶ │   Paired WRF simulations │
│    and LAI (2003–2020)   │          │ PHE2003–2005 / PHE2018–2020│
└──────────────────────────┘          └──────────────────────────┘
            │                                      │
            ▼                                      ▼
┌──────────────────────────┐          ┌──────────────────────────┐
│  Forest–cropland comparison│        │   TRM decomposition of   │
│    of phenological change │         │   temperature pathways   │
└──────────────────────────┘          └──────────────────────────┘
            │                                      │
             ╲                                    ╱
              ▼                                  ▼
        ┌──────────────────────────────────────────┐
        │  Implications for land-surface cooling,    │
        │ agricultural management, and regional planning│
        └──────────────────────────────────────────┘
```
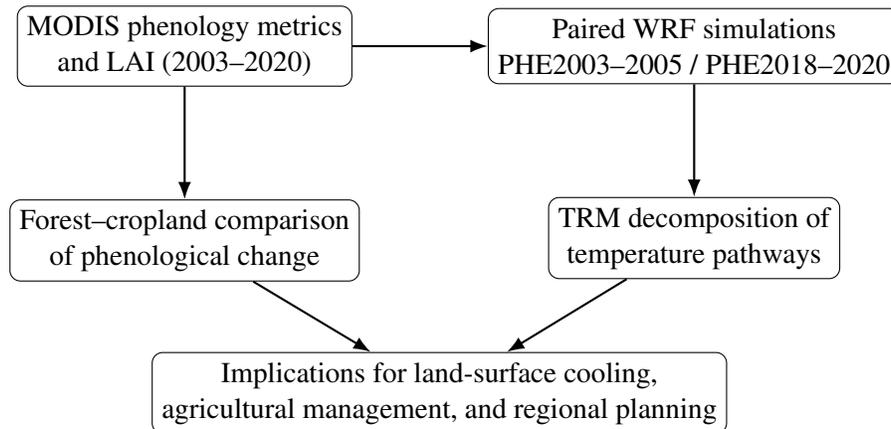
Figure 1: Analytical structure of the study. Long-term satellite phenology and canopy data are linked to paired regional climate simulations and pathway attribution to evaluate the planning significance of observed vegetation change.

DATA AND METHODS

Land-surface phenology and temperature datasets

Vegetation phenology was characterized using the MODIS MCD12Q2 Land Cover Dynamics product, which provides annual phenological metrics at 500 m resolution. The analysis used nine metrics describing the seasonal cycle, including green-up, mid-green-up, maturity, peak, senescence, mid-green-down, dormancy, minimum EVI, and maximum EVI. Annual values for these metrics were tracked over 2003–2020 to quantify directional change separately for forests and croplands. The length of season (LOS) was defined as the number of days between green-up and dormancy, and the seasonal canopy amplitude was represented as the difference between maximum and minimum EVI.

To represent continuous canopy development, the study used the MODIS MCD15A3H leaf area index (LAI) product, also at 500 m resolution. Four-day composite LAI values were interpolated to six-hour intervals to match the climate-model configuration and preserve consistent forcing across the paired simulations. Land-surface temperature (LST) was evaluated using the MODIS MYD11A2 product, while gridded near-surface air temperature was used to verify that the simulations reproduced the regional seasonal cycle before scenario differences were interpreted [4, 8, 17, 18]. Throughout the results, values reported with a ± term denote class-mean responses accompanied by the corresponding spatial spread across the contributing pixels.

Land-cover treatment

The analysis focused on stable forest and cropland pixels in order to isolate the climatic effects of phenology rather than conflating those effects with land-cover conversion. This restriction reduces a major source

of structural confounding in Northeast China, where climate trends and human land-use dynamics could otherwise affect the interpretation of temperature responses. By retaining only unchanged forest and cropland areas, the study preserves comparability across the 2003–2020 period and makes the subsequent forest–cropland contrast more interpretable.

Regional climate simulations

Regional simulations were performed using WRF version 4.2 with a 10 km horizontal resolution and a standard regional-climate configuration appropriate for Northeast China. Initial and boundary conditions were supplied by ERA5, and the paired design was implemented so that all model settings other than prescribed canopy trajectories remained fixed across experiments. One simulation used satellite-derived LAI representative of 2003–2005 (PHE2003–2005), and the other used LAI representative of 2018–2020 (PHE2018–2020). The simulations ran from July 1, 2015 to December 31, 2020, with the first six months used for spin-up and the subsequent five years used for analysis.

For croplands, this paired design is especially important because crop phenology is shaped by both climate and management. To isolate the thermal effect of phenological change, LAI was treated as the sole forcing difference between the two simulations, while other management assumptions, including irrigation and fertilization, were held constant [18]. Baseline model behavior was then interpreted against the observed seasonal evolution of LST and near-surface air temperature so that the reported scenario differences reflect a physically credible simulated climate state rather than an unconstrained numerical contrast. This means that the estimated temperature differences represent the biophysical influence of observed canopy-timing change, rather than the full combined effect of all agricultural change.

Biophysical attribution

To diagnose the mechanisms behind the LST response, the study uses the two-resistance mechanism (TRM) framework, which decomposes the surface temperature response into contributions from changes in surface albedo, aerodynamic resistance, surface resistance, emissivity, ground heat flux, and air-temperature feedback. The core decomposition can be written as

$$\Delta T_s = \frac{\partial T_s}{\partial \alpha}\Delta \alpha + \frac{\partial T_s}{\partial r_a}\Delta r_a + \frac{\partial T_s}{\partial r_s}\Delta r_s + \frac{\partial T_s}{\partial \varepsilon}\Delta \varepsilon + \frac{\partial T_s}{\partial G}\Delta G + \frac{\partial T_s}{\partial T_a}\Delta T_a. \qquad (1)$$

In this expression, ΔT_s is the LST change between the two phenology scenarios, and each term represents the contribution of a distinct biophysical pathway. The framework is particularly valuable because it separates direct land-surface changes from indirect atmospheric feedback, allowing the analysis to identify which mechanisms are most relevant for regional climate regulation [14, 18].

Consistent with the analytical design, mechanism attribution was restricted to pixels with LAI changes greater than 0.1 m^2 m^{-2} so that pathway interpretation focused on areas with substantively meaningful phenological change. This threshold reduces noise from near-zero vegetation differences and improves the interpretability of pathway shares.

Algorithm 1 Analytical workflow for phenology-induced temperature diagnosis

---

Require: MODIS phenology metrics, MODIS LAI, land-cover masks, WRF outputs for PHE2003–2005 and PHE2018–2020

Ensure: Phenology trends, monthly LST responses, and pathway attribution by land-cover class

1: Identify unchanged forest and cropland pixels
2: Compute annual phenology trends from 2003–2020 for each land-cover class
3: Construct early-period and late-period canopy trajectories from LAI observations
4: Run paired WRF simulations with identical settings except prescribed LAI
5: Subtract PHE2003–2005 from PHE2018–2020 to estimate monthly LST change
6: Apply the TRM framework to decompose ΔT_s into pathway-specific contributions
7: Compare forests and croplands in terms of timing, magnitude, and mechanism
8: Interpret the resulting seasonal temperature shifts in relation to planning and management

---

RESULTS

Phenology changed more strongly and more asymmetrically in croplands

The observational analysis shows clear but distinct phenological changes in forests and croplands. Forest phenology shifted primarily at the beginning and middle of the growing season. Mean forest green-up advanced by 0.39 days per year, mid-green-up by 0.38 days per year, maturity by 0.32 days per year, and peak by 0.37 days per year. Forest dormancy, by contrast, changed little, which means that forest growing-season extension was driven mainly by earlier spring development rather than by later autumn termination. Overall, forest LOS increased by 0.43 days per year.

Croplands exhibited a stronger and more spatially extensive reorganization of the seasonal cycle. Green-up advanced by 0.29 days per year and mid-green-up by 0.27 days per year, while mid-green-down was delayed by 0.24 days per year and dormancy by 0.42 days per year. This combined spring advancement and autumn delay produced a mean LOS increase of 0.71 days per year. Importantly, 59.15% of cropland LOS extension was attributable to delayed dormancy, which indicates that late-season persistence was a central feature of agricultural canopy change.

The same asymmetry appears in canopy amplitude. EVI amplitude increased significantly in both land-cover systems, but more strongly in croplands: $0.00283 \ \mathrm{yr}^{-1}$ in forests and $0.00435 \ \mathrm{yr}^{-1}$ in croplands. In cumulative terms, that corresponds to a 12% increase relative to the 2003 base value in forests and a 20% increase in croplands.

Table 1: Key observed phenology trends in Northeast China, 2003–2020

Metric	Forests	Croplands
Green-up trend (days yr^{-1})	−0.39	−0.29
Mid-green-up trend (days yr^{-1})	−0.38	−0.27
Maturity trend (days yr^{-1})	−0.32	−0.18
Peak trend (days yr^{-1})	−0.37	−0.06
Mid-green-down trend (days yr^{-1})	+0.04	+0.24
Dormancy trend (days yr^{-1})	+0.04	+0.42
Length of season trend (days yr^{-1})	+0.43	+0.71
EVI amplitude trend (yr^{-1})	+0.00283	+0.00435

Negative values indicate earlier timing (advancement); positive values indicate later timing (delay) or longer seasons.
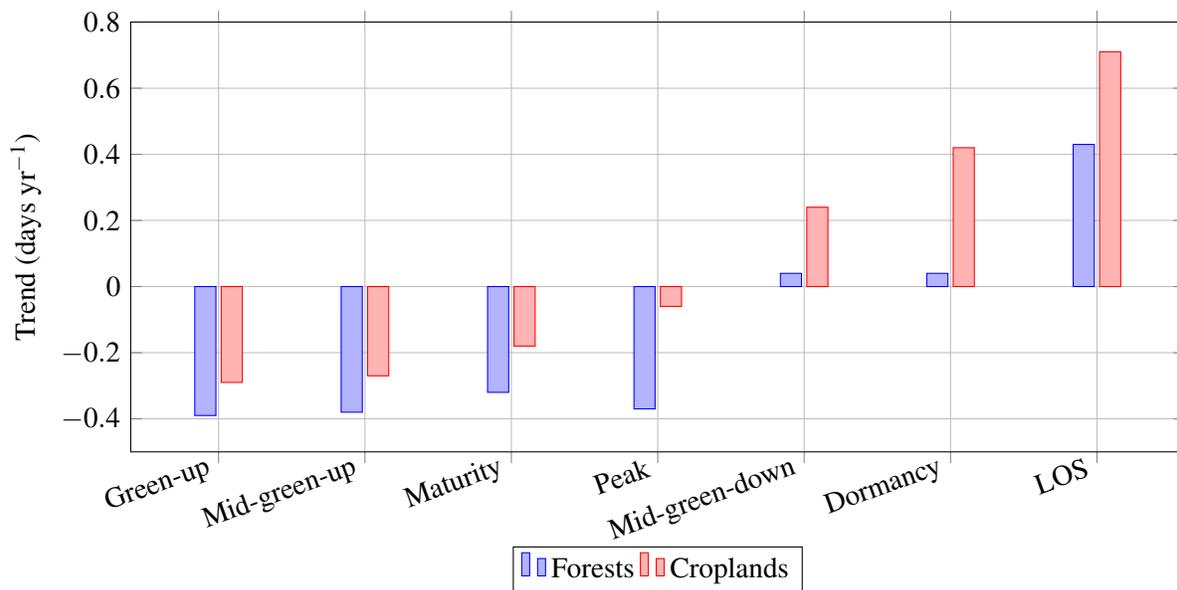
Figure 2: Observed phenology trends from 2003 to 2020. Croplands exhibit a stronger combined pattern of spring advancement and autumn delay, producing a larger extension of the active season than forests.

Phenological change cooled the surface more strongly in croplands

The paired WRF simulations indicate that phenological shifts altered LST primarily during the growing season. In forests, the response was seasonally concentrated. Earlier leaf-out increased forest LST by $0.07 \pm 0.06\,°C$ in April because the radiative effect of reduced snow albedo initially outweighed evapotranspirative cooling. Once canopy development intensified, however, the sign reversed: forest LST declined by $0.53 \pm 0.07\,°C$ in May, by $0.21 \pm 0.03\,°C$ in June, and by $0.08 \pm 0.03\,°C$ in July. Additional but smaller cooling persisted from August through October, with monthly declines in the range of 0.06–$0.09\,°C$.

Croplands showed a different seasonal pattern. Cooling was more persistent and aligned more closely with the core agricultural season. The largest reported declines occurred in June ($-0.47 \pm 0.15\,°C$), July ($-0.48 \pm 0.11\,°C$), and September ($-0.28 \pm 0.09\,°C$). This longer and more substantial cooling period reflects the combination of increasing canopy amplitude, substantial mid-season LAI growth, and delayed late-season

senescence in managed systems.

These differences are critical for planning interpretation. Forest phenology mainly altered spring temperature transitions, while cropland phenology reshaped the temperature profile during months more directly tied to crop development, field activity, and seasonal resource management.

Table 2: Selected monthly LST responses to observed phenology change

Land cover	Month	ΔLST (°C)	Interpretation
Forest	April	$+0.07 \pm 0.06$	Early spring warming
Forest	May	-0.53 ± 0.07	Strong green-up cooling
Forest	June	-0.21 ± 0.03	Moderate cooling
Forest	July	-0.08 ± 0.03	Weak cooling
Forest	Aug–Oct	-0.06 to -0.09	Persistent weak cooling
Cropland	June	-0.47 ± 0.15	Strong growing-season cooling
Cropland	July	-0.48 ± 0.11	Strong growing-season cooling
Cropland	September	-0.28 ± 0.09	Late-season cooling

Positive values indicate warming under the later-period phenology scenario; negative values indicate cooling.
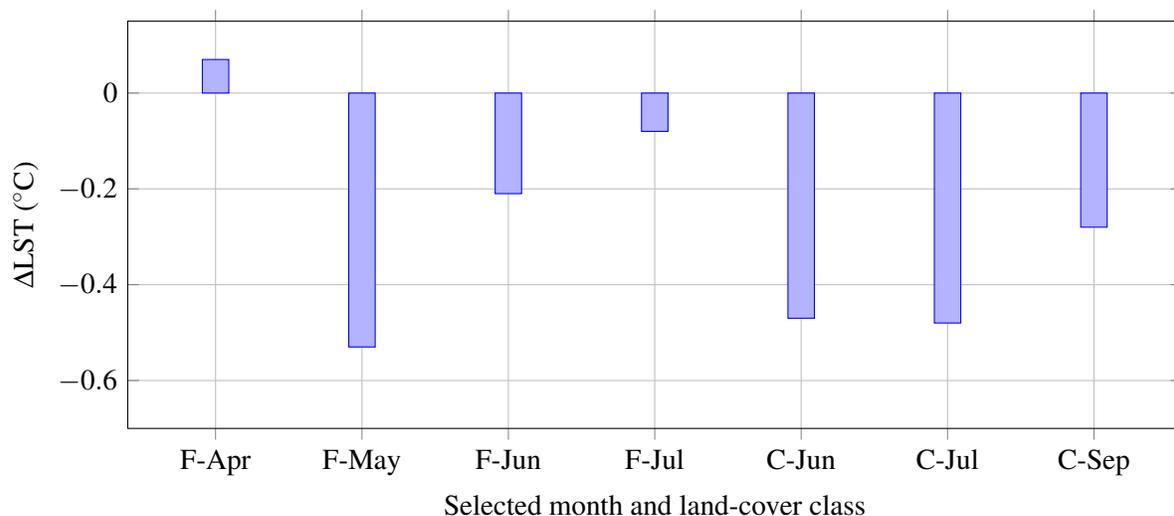

Figure 3: Selected reported monthly LST responses. Forest impacts are strongest in May, while cropland cooling is stronger and more persistent across the active agricultural season.

Croplands exhibited higher LST sensitivity to LAI

The analysis further shows that the cooling impact of phenology depends not only on the magnitude of LAI change but also on the sensitivity of LST to a given unit of LAI increase. On this metric, croplands were markedly more responsive than forests. This sensitivity contrast provides an internal consistency check on the simulated temperature response by showing that stronger cropland cooling is supported by both larger canopy change and a larger thermal response per unit LAI.

The growing-season mean LST sensitivity to LAI was -0.33 °C m^2 m^{-2} in forests and -0.84 °C m^2 m^{-2} in croplands. In other words, the same unit increase in LAI produced substantially more cooling in croplands.

Sensitivity was also strongly seasonal. In forests, the largest sensitivities occurred in October ($-0.62 \pm 0.49\,°\text{C m}^2\,\text{m}^{-2}$) and May ($-0.55 \pm 0.42\,°\text{C m}^2\,\text{m}^{-2}$). In croplands, the strongest sensitivities occurred in May ($-1.67 \pm 0.70\,°\text{C m}^2\,\text{m}^{-2}$) and June ($-1.33 \pm 0.73\,°\text{C m}^2\,\text{m}^{-2}$), followed by October and September.

This result clarifies why July cropland cooling was so large: the July sensitivity itself was smaller ($-0.46 \pm 0.40\,°\text{C m}^2\,\text{m}^{-2}$), but July also had the largest LAI increase ($1.10\,\text{m}^2\,\text{m}^{-2}$), so the product of sensitivity and canopy change still produced strong net cooling.

Aerodynamic resistance was the dominant pathway, with atmospheric feedback close behind

Biophysical decomposition shows that reduced aerodynamic resistance (r_a) was the principal mechanism of cooling in both land-cover systems. Averaged across the growing season, aerodynamic resistance contributed $-0.16 \pm 0.13\,°\text{C m}^2\,\text{m}^{-2}$ in forests and $-0.34 \pm 0.20\,°\text{C m}^2\,\text{m}^{-2}$ in croplands, accounting for 53% and 51% of the total biophysical cooling signal, respectively.

The second most important contribution came from air-temperature feedback (T_a), which accounted for $-0.15 \pm 0.18\,°\text{C m}^2\,\text{m}^{-2}$ (46%) in forests and $-0.29 \pm 0.25\,°\text{C m}^2\,\text{m}^{-2}$ (38%) in croplands. This result matters because it shows that the cooling signal was not purely a local land-surface phenomenon. Once vegetation altered roughness and energy exchange, the atmosphere responded in ways that further influenced surface temperature.

Other pathways were comparatively small. In forests, albedo, surface resistance, emissivity, and ground heat flux were negligible relative to the dominant terms. In croplands, surface albedo and surface resistance were somewhat more relevant, contributing 6% and 5%, respectively, but they remained secondary compared with aerodynamic resistance and atmospheric feedback.

Table 3: LST sensitivity and dominant pathway contributions

| Metric	Forests	Croplands
Growing-season mean $\partial T_s/\partial\text{LAI}$ ($°\text{C m}^2\,\text{m}^{-2}$)	-0.33	-0.84
Largest reported monthly sensitivity ($°\text{C m}^2\,\text{m}^{-2}$)	-0.62 ± 0.49 (Oct)	-1.67 ± 0.70 (May)
Aerodynamic resistance contribution	-0.16 ± 0.13	-0.34 ± 0.20
Aerodynamic resistance share (%)	53	51
Air-temperature feedback contribution	-0.15 ± 0.18	-0.29 ± 0.25
Air-temperature feedback share (%)	46	38
Surface albedo share (%)	negligible	6
Surface resistance share (%)	negligible	5
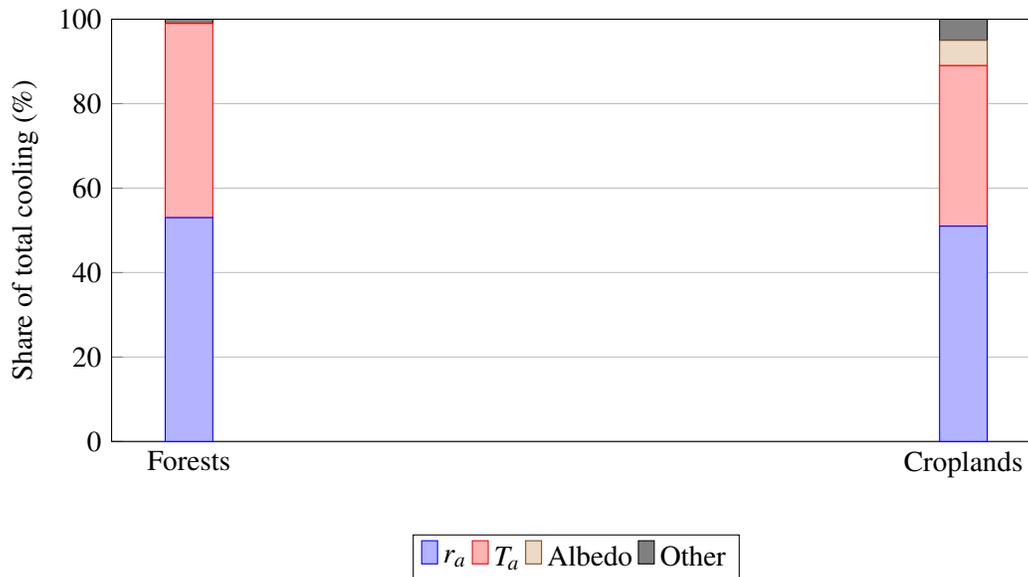
Figure 4: Growing-season shares of the biophysical cooling signal. Reduced aerodynamic resistance is the dominant pathway, but atmospheric feedback also carries substantial weight, especially at the regional scale.

MANAGEMENT AND PLANNING IMPLICATIONS

The empirical results have direct relevance for management and planning in climate-sensitive agricultural regions, but the evidence is most appropriately interpreted as a biophysical constraint rather than as a direct estimate of economic or agronomic performance.

First, the findings identify crop phenology as a practical determinant of regional thermal conditions. Because cropland cooling is stronger and more persistent than forest cooling during the active growing season, agricultural timing is not simply a response to climate; it also modulates part of the surface process that shapes seasonal temperature. This means that crop calendars, cultivar maturity profiles, sowing strategies, and management practices that influence canopy timing can alter the thermal background against which agricultural operations take place.

Second, the asymmetry between forests and croplands implies that land-cover class matters for adaptation planning. Forest systems predominantly affect the spring transition, which is relevant for snowmelt, seasonal onset, and ecological monitoring. Cropland systems, by contrast, affect temperature during June, July, and September—months that are far more central to grain filling, field labor, and late-season production decisions. For regional planners, this means that the timing of vegetation cooling should be matched to the timing of sectoral exposure.

Third, the prominence of atmospheric feedback indicates that planners should avoid treating vegetation effects as purely local. Once canopy development changes, the atmosphere responds. The practical implication is that land-use planning, agricultural planning, and climate adaptation planning cannot be treated as fully separable at regional scale. Changes in vegetation timing can influence boundary-layer conditions and therefore modify the local expression of seasonal warming.

Fourth, because cropland dormancy delay was a major component of growing-season extension, late-season management deserves greater analytical attention in adaptation strategies. In this study, autumn canopy persistence was not a marginal phenomenon; it was a central reason that croplands exhibited stronger cooling

and longer seasonal influence than forests. This makes late-season canopy maintenance, harvest timing, and residue decisions plausible components of climate-responsive planning.

DISCUSSION

The study supports three main conclusions.

The first is that phenological change in Northeast China was not uniform across land-cover systems. Forests advanced mainly in spring, while croplands combined earlier spring development with later autumn shutdown. This asymmetry matters because it changes not only the total growing-season length, but also the seasonal placement of land–atmosphere interactions.

The second is that croplands exerted stronger cooling influence than forests under the observed phenological changes. This occurred because croplands combined larger canopy-amplitude increases with stronger LST sensitivity and a more seasonally persistent phenological shift. The contrast is especially important in a region where agricultural land is strategically important and where management decisions can modify canopy trajectories.

The third is mechanistic: the cooling signal was driven mainly by aerodynamic resistance, but it cannot be understood without accounting for atmospheric feedback. This means that the climate effects of vegetation change are partly emergent properties of coupled land–atmosphere dynamics. In methodological terms, this supports the use of fully coupled regional simulations rather than simpler offline surface-energy approaches when the research objective is to understand operationally meaningful climate impacts.

Taken together, the observational trends, paired-simulation contrasts, and pathway decomposition provide mutually reinforcing evidence. The main conclusions do not depend on a single indicator; they are supported by aligned changes in timing, canopy magnitude, temperature response, and physical mechanism.

At the same time, the interpretation has limits. Because the simulations held management practices constant and changed only LAI, the reported temperature effects isolate phenology-related biophysical forcing rather than the entire real-world effect of agricultural transformation. That is a strength for causal clarity, but it also means that the results should not be overextended into claims about total agronomic or socioeconomic outcomes. Likewise, the regional 10 km grid captures broad climate responses, not field-scale heterogeneity.

Even with these limits, the planning significance is clear. In a warming agricultural region, vegetation timing is part of the system through which climate risk is mediated. Ignoring phenology in planning models would therefore omit a measurable component of the regional thermal regime.

CONCLUSION

This study shows that vegetation phenology is a meaningful regulator of seasonal land-surface temperature in Northeast China and that its effects are stronger in croplands than in forests. From 2003 to 2020, forests experienced earlier spring development, while croplands combined earlier green-up with later dormancy, producing a larger extension of the active season in managed land. These shifts increased canopy development and intensified vegetation–climate interactions.

The temperature response was land-cover specific. Forests showed their strongest cooling in May, after a brief April warming linked to snow–albedo effects. Croplands produced stronger and more persistent cooling during the main agricultural season, with the clearest reported declines in June, July, and September. The

mechanism analysis showed that reduced aerodynamic resistance was the dominant cooling pathway, while atmospheric feedback was the second most important contributor.

For management and planning, the implication is that phenology should be treated as a climate-relevant operational variable. In large agricultural regions, shifts in canopy timing can alter seasonal temperature conditions in ways that matter for adaptation planning, land-use decisions, and the interpretation of regional climate risk. Climate-responsive planning should therefore incorporate dynamic vegetation timing rather than assume a static seasonal land surface.

ACKNOWLEDGEMENTS

DATA AVAILABILITY STATEMENT

The primary inputs used in this study are publicly available satellite and reanalysis products identified in the Methods. Processed derivatives used to generate the reported summaries can be made available by the corresponding author upon reasonable request, subject to journal data-sharing requirements.

REFERENCES

[1] Bonan, G.B. (2008). Forests and climate change: forcings, feedbacks, and the climate benefits of forests. *Science*, 320(5882), 1444–1449.

[2] Bright, R.M., Davin, E., O'Halloran, T., Pongratz, J., Zhao, K.-G., and Cescatti, A. (2017). Local temperature response to land cover and management change driven by non-radiative processes. *Nature Climate Change*, 7, 296–302.

[3] Chen, C., Park, T., Wang, X., Piao, S., Xu, B., Chaturvedi, R.K., Fuchs, R., Brovkin, V., Ciais, P., and Fensholt, R. (2019). China and India lead in greening of the world through land-use management. *Nature Sustainability*, 2, 122–129.

[4] Friedl, M.A. and Sulla-Menashe, D. (2022). *MCD12Q2 MODIS/Terra+Aqua Land Cover Dynamics Yearly L3 Global 500m SIN Grid, Version 6.1*. NASA LP DAAC.

[5] Graven, H.D., Keeling, R.F., Piper, S.C., Patra, P.K., Stephens, B.B., Wofsy, S.C., Welp, L.R., Sweeney, C., Tans, P.P., and Kelley, J.J. (2013). Enhanced seasonal exchange of CO_2 by northern ecosystems since 1960. *Science*, 341(6150), 1085–1089.

[6] Hersbach, H., Bell, B., Berrisford, P., Hirahara, S., Muñoz-Sabater, J., Nicolas, J., Peubey, C., Radu, R., Schepers, D., and Simmons, A. (2020). The ERA5 global reanalysis. *Quarterly Journal of the Royal Meteorological Society*, 146, 1999–2049.

[7] Lian, X., Piao, S., Li, L.Z.X., Huntingford, C., Ciais, P., Peng, S., Zeng, Z., and Wang, X. (2020). Summer soil drying in northern ecosystems linked to earlier spring greening. *Nature Climate Change*, 10, 164–170.

[8] Myneni, R.B., Knyazikhin, Y., and Park, T. (2021). *MCD15A3H MODIS/Terra+Aqua Leaf Area Index/FPAR 4-Day L4 Global 500m SIN Grid, Version 6.1*. NASA LP DAAC.

[9] Niu, G.-Y., Yang, Z.-L., Mitchell, K.E., Chen, F., Ek, M.B., Barlage, M., Kumar, A., Manning, K., Niyogi, D., and Rosero, E. (2011). The community Noah land surface model with multiparameterization options (Noah-MP). *Journal of Geophysical Research*, 116, D12109.

[10] Park, H. and Jeong, S. (2023). Vegetation phenology and its climatic feedbacks across seasons and biomes. *Current Climate Change Reports*, 9, 90–104.

[11] Peñuelas, J., Rutishauser, T., and Filella, I. (2009). Phenology feedbacks on climate change. *Science*, 324(5929), 887–888.

[12] Piao, S., Tan, J., Chen, A., Fu, Y.H., Ciais, P., Liu, Q., Janssens, I.A., Vicca, S., Zeng, Z., and Jeong, S.-J. (2015). Leaf onset in the northern hemisphere triggered by daytime temperature. *Nature Communications*, 6, 6911.

[13] Piao, S., Liu, Q., Chen, A., Janssens, I.A., Fu, Y.H., Dai, J., Liu, L., Lian, X., Shen, M., and Zhu, X. (2019). Plant phenology and global climate change: current progresses and challenges. *Global Change Biology*, 25, 1922–1940.

[14] Rigden, A.J. and Li, D. (2017). Attributing surface temperature sensitivity to vegetation change through aerodynamic and surface resistances. *Journal of Climate*, 30, 4789–4804.

[15] Skamarock, W.C., Klemp, J.B., Dudhia, J., Gill, D.O., Liu, Z., Berner, J., Wang, W., Powers, J.G., Duda, M.G., Barker, D.M., and Huang, X.-Y. (2019). *A Description of the Advanced Research WRF Model, Version 4*. NCAR Technical Note.

[16] Stéfanon, M., Drobinski, P., D'Andrea, F., and de Noblet-Ducoudré, N. (2012). Effects of interactive vegetation phenology on the 2003 summer heat waves. *Journal of Geophysical Research*, 117, D24103.

[17] Wan, Z., Hook, S., and Hulley, G. (2015). *MYD11A2 MODIS/Aqua Land Surface Temperature/Emissivity 8-Day L3 Global 1km SIN Grid, Version 6*. NASA LP DAAC.

[18] Yu, L., Liu, Y., Yan, F., Lu, L., Li, X., Zhang, S., and Yang, J. (2025). Phenological control of vegetation biophysical feedbacks to the regional climate. *Geography and Sustainability*, 6, 100202.

Emily Jones, School of Design, California State University Long Beach, Long Beach, CA 90840, United States